Hind III digestion released another band of 5 kb, consisting largely of pBSKS vector sequences (Fig. 2A). Circularization of Hind III–digested genomic DNA containing pMD223 integrated by homologous recombination into a genomic array of 2.3-kb repeats will result in the formation of circular DNA elements that can be rescued by transformation back into *E. coli*. Digestion of rescued plasmid with Hind III and Eco RI demonstrates the rescue of the Hind III site adjacent to the site of integration and distinguishes between integrated and episomally maintained vector because the latter contains an additional 1.2-kb fragment (Fig. 2B). Sequence analysis confirmed the rescue of the Hind III site, which delineates the termini of the 2.3-kb repeat (*5*).

7. M. Lanzer, D. de Bruin, J. V. Ravetch, *Nature* **361**, 654 (1993).
8. M. Lanzer, K. Fischer, S. M. Le Blancq, *Mol. Biochem. Parasitol.* **70**, 1 (1995).
9. S. L. Gerring, C. Connelly, P. Hieter, *Methods Enzymol.* **194**, 57 (1991).
10. P. Borst and D. R. Greaves, *Science* **235**, 658 (1987).
11. L. G. Pologe and J. V. Ravetch, *Cell* **55**, 869 (1988); L. G. Pologe, D. de Bruin, J. V. Ravetch, *Mol. Cell. Biol.* **10**, 3243 (1990); A. Scherf *et al.*, *EMBO J.* **11**, 2293 (1992).
12. T. Pace *et al.*, *Mol. Cell. Biol.* **10**, 6759 (1990); C. J. Janse, J. Ramesar, B. Mons, *Nucleic Acids Res.* **20**, 581 (1992); E. Dore, T. Pace, M. Ponzi, L. Picci, C. Frontali, *Mol. Cell. Biol.* **10**, 2423 (1990); M. Ponzi *et al.*, *Nucleic Acids Res.* **20**, 4491 (1992).
13. During the course of this work we became aware of similar work with asexual bloodstage forms of the human malaria parasite, *P. falciparum*. Plasmid DNA has been successfully introduced into the *P. falciparum* genome in a site-specific manner with DHFR-TS genes from either *P. falciparum* or *Toxoplasma gondii*. A manuscript describing this work is now in press (Y. Wu, L. A. Kirkman, T. E. Wellems, *Proc. Natl. Acad. Sci. U.S.A.*, in press.
14. We thank J. Ramesar and J. Kos for technical assistance, the yeast genetics group in the Institute of Molecular Plant Sciences at Leiden for consideration of our work, R. Vinkenoog and R. E. Sinden for discussions, G. van Dam for curve fitting, and H. A. del Portillo for critical reading of the manuscript. This work was supported by grants from the European Union program "Science and Technology for Development" (contract TS3*-CT92-0116) and the United Nations Development Program–World Bank–World Health Organization Special Programme in Research and Training in Tropical Diseases (contract 940351).

11 August 1995; accepted 21 November 1995

IRS-1–Mediated Inhibition of Insulin Receptor Tyrosine Kinase Activity in TNF-α– and Obesity-Induced Insulin Resistance

Gökhan S. Hotamisligil,* Pascal Peraldi, Adriane Budavari, Ramsey Ellis, Morris F. White, Bruce M. Spiegelman†

Tumor necrosis factor–α (TNF-α) is an important mediator of insulin resistance in obesity and diabetes through its ability to decrease the tyrosine kinase activity of the insulin receptor (IR). Treatment of cultured murine adipocytes with TNF-α was shown to induce serine phosphorylation of insulin receptor substrate 1 (IRS-1) and convert IRS-1 into an inhibitor of the IR tyrosine kinase activity in vitro. Myeloid 32D cells, which lack endogenous IRS-1, were resistant to TNF-α–mediated inhibition of IR signaling, whereas transfected 32D cells that express IRS-1 were very sensitive to this effect of TNF-α. An inhibitory form of IRS-1 was observed in muscle and fat tissues from obese rats. These results indicate that TNF-α induces insulin resistance through an unexpected action of IRS-1 to attenuate insulin receptor signaling.

Insulin resistance, a smaller than normal response to a given amount of insulin, is a common pathological state frequently associated with a number of diseases, including chronic infection, cancer, and obesity (*1*, *2*). In the case of obesity, insulin resistance is a ubiquitous correlate and predisposes the obese individual to the most deleterious consequences of this condition, such as cardiovascular complications and, especially, non–insulin-dependent diabetes mellitus (NIDDM) (*3*). However, the molecular mechanisms responsible for the development of insulin resistance in obesity are not well understood.

Overexpression of TNF-α from adipose tissue is a common feature of many different rodent models of obesity (*4*, *5*). Increased TNF-α expression in adipose tissue is also present in human obesity and correlates with the extent of obesity and the level of hyperinsulinemia, an indirect measure of insulin resistance (*6*). Moreover, neutralization of TNF-α in obese and insulin-resistant rats improves IR signaling and insulin sensitivity of peripheral tissues, demonstrating that TNF-α interferes with insulin action in this disease (*4*, *7*).

Binding of insulin stimulates the intrinsic tyrosine kinase of the IR, which results in autophosphorylation of the β subunits on tyrosine residues and subsequent phosphorylation of insulin receptor substrate 1 (IRS-1) (*8*). One mechanism by which TNF-α interferes with insulin action is through its ability to inhibit these proximal steps in IR signaling in both cultured cells and whole animals (*7*, *9*, *10*). Treatment of adipose cells with TNF-α produces a decrease in both insulin-stimulated IR autophosphorylation and subsequent tyrosine phosphorylation of IRS-1 (*9*). Similar results have also been obtained with cultured hepatoma cells, muscle cells, and fibroblasts (*10*–*12*). The time course of TNF-α effects on IR signaling, however, is variable in these different cell types.

TNF-α initiates a cascade of signal transduction events through the activation of multiple protein kinases (*13*). We therefore examined whether TNF-α also induces alterations in the phosphorylation of IR or IRS-1 or both. We metabolically labeled 3T3-F442A adipocytes with [^{32}P]orthophosphate and determined the phosphorylation patterns of IR and IRS-1 before and after TNF-α treatment. As expected, insulin-stimulated autophosphorylation of the IR and phosphorylation of IRS-1 were reduced in TNF-α–treated adipocytes (Fig. 1A). An increase (≈threefold) in IRS-1 phosphorylation was apparent in TNF-α–treated cells compared with the controls. There was no detectable tyrosine phosphorylation of IRS-1 without insulin stimulation. However, we observed two proteins, p120 and p210, that were tyrosine phosphorylated upon TNF-α stimulation. The identity of these proteins is currently unknown. Phosphoamino acid analysis of IRS-1 isolated from control and TNF-α–treated cells revealed that the TNF-α–induced phosphorylation of IRS-1 occurred exclusively on serine residues (Fig. 1C). No phosphorylation of IRS-1 was detected in control adipocytes.

Phosphorylation of IRS-1 on serine and threonine residues interferes with the subsequent insulin-stimulated tyrosine phosphorylation of IRS-1 by the IR (*14*). Treatment of adipocytes with okadaic acid, a protein phosphatase inhibitor, which results in increased serine and threonine phosphorylation of IRS-1, also reduces the capacity of IRS-1 to be phosphorylated by the IR and induces a state of cellular insulin resistance (*14*). We therefore asked whether the serine-phosphorylated IRS-1 from TNF-α–treated cells can be phosphorylated normally by the IR after insulin stimulation. IRS-1 was immunoprecipitated from control and TNF-α–treated cells and incorporated in an in vitro kinase assay with par-

G. S. Hotamisligil, P. Peraldi, A. Budavari, R. Ellis, B. M. Spiegelman, Department of Cellular and Molecular Biology, Dana-Farber Cancer Institute, and Department of Cell Biology, Harvard Medical School, 44 Binney Street, Boston, MA 02115, USA.
M. F. White, Joslin Diabetes Center and Department of Medicine, Harvard Medical School, Boston, MA 02215, USA.

*Present address: Department of Nutrition, Harvard School of Public Health, 665 Huntington Avenue, Boston, MA 02115, USA.
†To whom correspondence should be addressed. E-mail: bruce_spiegelman@dfci.harvard.edu

tially purified IRs from untreated 3T3-F442A adipocytes. Insulin-stimulated phosphorylation of IRS-1 isolated from TNF-α–treated adipocytes was reduced (40 to 60% in three experiments) compared with the IRS-1 isolated from control cells (Fig. 2). To test whether this decrease in insulin-stimulated phosphorylation was the result of TNF-α–induced serine phosphorylation of IRS-1, we incubated the IRS-1 samples with calf intestinal alkaline phosphatase before adding the samples to the in vitro kinase assay. This treatment resulted in a recovery of IRS-1 phosphorylation upon insulin stimulation, whereas heat-inactivated alkaline phosphatase had no effect. These results suggest that TNF-α–induced phosphorylation of IRS-1 is an important component underlying the reduced capacity of IRS-1 for accepting insulin-induced phosphorylation (Fig. 2).

Given the well-established role of IRS-1 in signaling downstream from the IR, the reduced insulin-stimulated phosphorylation of IRS-1 as a result of the TNF-α–induced modification can theoretically explain some of the defective IR signaling in TNF-α–treated cells. However, TNF-α treatment reduces both insulin-stimulated IR autophosphorylation and phosphorylation of IRS-1 (*9*, *10*) (Fig. 1). We therefore considered the possibility that the modified IRS-1 might not only interfere with propagation of insulin signaling downstream of the IR, but might impair the activity of the IR tyrosine kinase. We examined the insulin-stimulated autophosphorylation of the partially purified IR in the presence of IRS-1 isolated from control and TNF-α–treated adipocytes. We observed a decrease (60 ± 14% in five experiments) in insulin-stimulated IR autophosphorylation when exogenous IRS-1 from TNF-α–treated cells was added to the kinase assay (Fig. 3A). This effect appeared to be specific for IRS-1, because no differences were detectable when comparable immunoprecipitations were prepared from control and TNF-α–treated cells with preimmune serum or protein A–Sepharose beads alone (Fig. 3A). The quantity of IRS-1 protein added from the control or TNF-α–treated cells was similar (Fig. 3). The decrease in insulin-stimulated IR autophosphorylation was evident at all time points between 5 and 30 min (*12*), indicating a difference in the absolute rate of IR autophosphorylation in the presence of IRS-1 from TNF-α–treated cells.

Incubation of immunoprecipitated IRS-1 with calf intestinal alkaline phosphatase before the kinase reaction resulted in the loss of the inhibitory action of IRS-1 toward the insulin-stimulated IR autophosphorylation, and this effect was observed at all time points examined (Fig. 3B). These results demonstrate that after its phosphorylation resulting from treatment with TNF-α, IRS-1 acquires an inhibitory activity toward the IR tyrosine kinase.

We also studied the effect of TNF-α on IR signaling in the myeloid 32D cell line which lacks endogenous IRS-1 and the related protein IRS-2/4PS (*15*). To monitor the involvement of IRS-1 in TNF-α–mediated inhibition of IR signaling, we used 32D cell lines that ectopically express only the IR (32D-IR) or both the IR and IRS-1 (32D-IR + IRS-1) and examined insulin-stimulated IR phosphorylation after treatment of the cells with TNF-α. In cells expressing only the IR, the amount of insulin-stimulated tyrosine phosphorylation of the β subunit was unaffected by TNF-α at doses ranging from 0.5 to 100 ng/ml (Fig. 4). In contrast, in 32D cells expressing both IR and IRS-1, TNF-α treatment resulted in inhibition of insulin-stimulated IR autophosphorylation. Diminished insulin-stimulated IR autophosphorylation was apparent in these cells at TNF-α doses as low as 0.5 ng/ml and was ≈80% at 100 ng/ml (Fig. 4). Insulin-stimulated IRS-1 phosphorylation was also reduced after TNF-α treatment of these cells (*12*). The amount of IR protein was not changed under these conditions (Fig. 4). These data provided genetic evidence that the inhibition of IR signaling by TNF-α is dependent on the presence of IRS-1 in intact cells.

In obese animals, TNF-α plays a key role in abnormal IR signaling and systemic insulin resistance (*4*, *7*). We therefore asked whether an inhibitory form of IRS-1 was present in tissues of obese and insulin-resistant animals. We examined the insulin-stimulated autophosphorylation of partially purified IR in the presence of IRS-1 isolated from tissues of lean and obese fa/fa rats. Insulin-stimulated IR autophosphorylation was reduced in the presence of IRS-1 isolated from fat (40 to 50%) and muscle (30 to 40%) tissues of obese animals compared with that in the presence of IRS-1 from lean controls (Fig. 5A). In contrast, little or no difference was observed in IR autophosphorylation when IR was incubated with

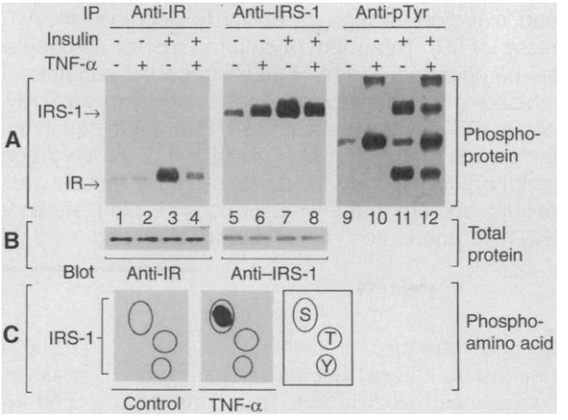

Fig. 1. TNF-α effects on (**A**) basal and insulin-stimulated phosphorylation of insulin receptor (IR) and insulin receptor substrate 1 (IRS-1), (**B**) total protein quantity of IR and IRS-1, and (**C**) phosphoamino acid composition of IRS-1 in cultured adipocytes. 3T3-F442A adipocytes were grown and differentiated as described (*9*). Control and TNF-α–treated adipocytes (*19*) were metabolically labeled with radioactive orthophosphate, stimulated with insulin, and protein extracts were prepared as described (*9*). Immunoprecipitations (IP) were then done with polyclonal antibodies to IR and IRS-1 and a monoclonal antibody to phosphotyrosine (anti-pTyr). Proteins were resolved by SDS-PAGE (7.5% polyacrylamide), transferred to nitrocellulose, and identified by autoradiography. The same filters were used to determine IR and IRS-1 protein concentrations by protein immunoblot analysis (Blot) (*9*). For two-dimensional phosphoamino acid analysis, proteins were blotted on Immobulon membranes (Millipore); the IRS-1 bands were isolated after autoradiography and analyzed as described (*20*). The predicted migration patterns of the respective amino acids are indicated (S, serine; T, threonine; and Y, tyrosine).

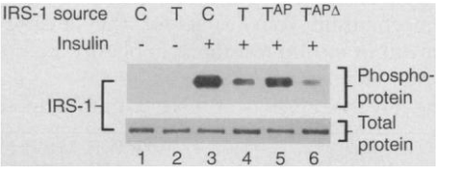

Fig. 2. Reduced IR-mediated phosphorylation of IRS-1 obtained from TNF-α–treated cells. IRS-1 was immunoprecipitated from total cellular extracts (5 mg) prepared from control (C) or TNF-α–treated (T) adipocytes (*9*). Immunoprecipitates of IRS-1 were resuspended in tris-EDTA buffer and incubated with active (lane T^{AP}) or heat-inactivated (lane $T^{AP\Delta}$) calf intestinal alkaline phosphatase (20 U, as described by Stratagene) for 30 min at 25°C for dephosphorylation reactions, washed five times with RIPA buffer [150 mM NaCl, 10 mM phosphate buffer (pH 7.0), 1% NP-40, 1% sodium deoxycholate, 0.1% sodium lauryl sulfate], and resuspended in 20 μl of reaction buffer A [50 mM Hepes (pH 7.6), 0.025% Triton X-100, 5 mM $MnCl^{2+}$, and 50 μM adenosine triphosphate (ATP)]. Insulin receptors were partially purified by wheat-germ (Vector Labs, California) affinity chromatography from fully differentiated control 3T3-F442A adipocytes as described (*9*), activated by insulin in the presence of 5 mM $MnCl^{2+}$, 50 μM ATP, and 20 μCi [γ-^{32}P]ATP, and incubated with immunoprecipitated IRS-1 from control or TNF-α–treated cells for 30 min. The reactions were stopped by addition of Laemmli buffer followed by boiling for 2 min. The samples were analyzed by SDS-PAGE followed by autoradiography.

IRS-1 immunoprecipitated from liver or spleen (Fig. 5A). This inhibitory action of IRS-1 obtained from fat and muscle tissues of obese animals was prevented by enzymatic dephosphorylation of the IRS-1 before the kinase assay (Fig. 5B). These data show that an inhibitory form of IRS-1 is associated with precisely those tissues from obese animals in which TNF-α has been causally linked to insulin resistance. Taken together with previous data, these results strongly suggest that insulin resistance in obesity is, at least in part, the result of TNF-α–induced inhibition of IR signaling mediated by a modified form of IRS-1.

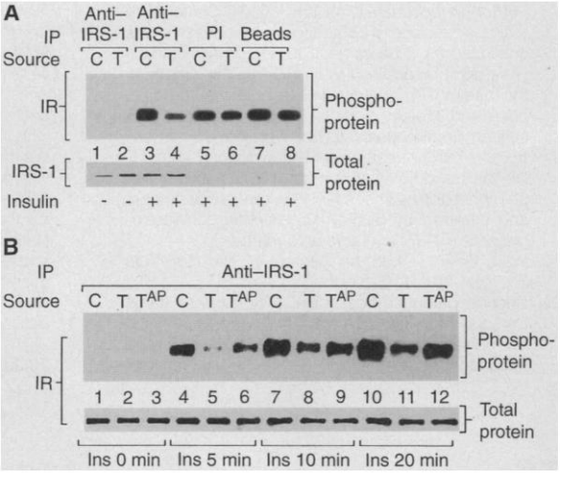

Fig. 3. Inhibitory effect of IRS-1 from TNF-α–treated cells on insulin-stimulated IR autophosphorylation (**A**) and removal of this inhibitory effect through dephosphorylation of IRS-1 (**B**). IRS-1 was immunoprecipitated from total cellular extracts (5 mg) prepared from control (C) or TNF-α–treated (T) adipocytes with a polyclonal antibody to IRS-1 (anti–IRS-1) or with preimmune serum (PI) or protein A–Sepharose (Pharmacia) beads alone. Dephosphorylation of IRS-1 immunoprecipitates was done as described (Fig. 2). Partially purified IRS from fully differentiated control 3T3-F442A adipocytes were activated by insulin for 15 min at 25°C and incubated with immunoprecipitated IRS-1 from control or TNF-α–treated cells in the presence of 5 μM ATP and 20 μCi [γ-^{32}P]ATP for 15 min (A) or as indicated (B). The reactions were stopped by the addition of Laemmli buffer followed by boiling for 2 min. The proteins were then resolved by SDS-PAGE, transferred to nitrocellulose membranes, and analyzed by autoradiography. Protein quantities of IR and IRS-1 were measured by protein immunoblot analysis of the same filters with polyclonal antibodies to both proteins.

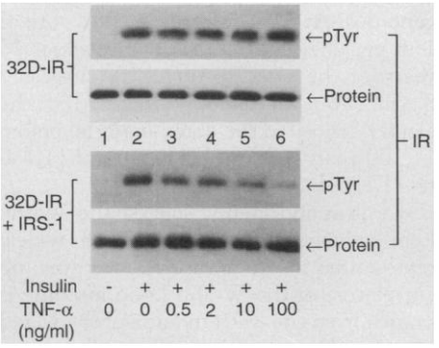

Fig. 4. Effect of TNF-α on IR tyrosine phosphorylation in 32D-IR and 32D-IR + IRS-1 cells. 32D cells (*16*) were grown in suspension in RPMI 1640 medium, supplemented with bovine calf serum (10%) and WEHI-3 conditioned media (5%) as a source of interleukin-3 as described (*15*). Cells (2×10^7) were treated for 4 hours with the indicated doses of TNF-α, stimulated with insulin (500 ng/ml, +) for 3 min, washed in ice-cold PBS, and lysed in a buffer containing 1% Triton X-100, 150 mM NaCl, 50 mM Hepes (pH 7.4), 10 mM EDTA, 100 mM NaF, 10 mM $Na_4P_2O_7$, 2 mM Na_3VO_4, 10 mM benzamidine, 2 mM PMSF, 20 mM leupeptine, and aprotinin (100 μg/ml). Cell viability was tested with trypan blue exclusion at all TNF-α doses. The IRs were immunoprecipitated for 90 min at 4°C and analyzed by immunoblotting with antibodies to phosphotyrosine (pTyr) or the IR. This experiment is representative of four experiments that gave similar results.

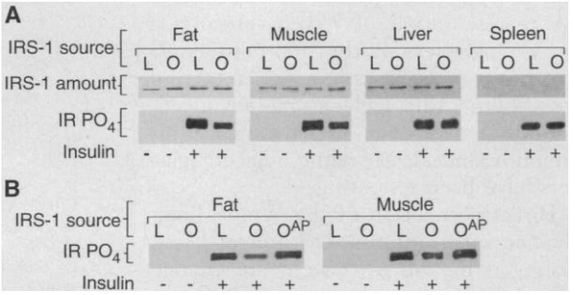

Fig. 5. Effects of IRS-1 from various tissues of obese fa/fa rats on insulin-stimulated IR autophosphorylation (**A**) Protein extracts from fat, muscle, liver, and spleen tissues of lean (L) and obese (O) 11- to 12-week-old male Zucker rats were prepared as described (*21*). IRS-1 was immunoprecipitated from total tissue extracts (5 mg) with a polyclonal antibody to IRS-1. IR autophosphorylation and protein quantities were determined as described (Fig. 3). (**B**) Removal of the inhibitory action of IRS-1 from obese fat and muscle tissues by dephosphorylation. IRS-1 immunoprecipitates were dephosphorylated with calf intestinal alkaline phosphatase before addition to the in vitro kinase assay as described (Fig. 2), and insulin-stimulated IR autophosphorylation was measured. Protein quantities were determined by protein immunoblot analysis as described (Fig. 3).

TNF-α is centrally important in animal models of obesity and insulin resistance (*2*). It is overexpressed from the fat of many animal models of obesity–NIDDM (*4, 5*) and is expressed in increased amounts from the fat of obese insulin-resistant humans (*6*). It plays a key role in the suppression of insulin action through its ability to inhibit IR signaling, as evidenced by neutralization experiments (*4, 7, 9*). TNF-α can also regulate the cellular quantity of Glut4, as demonstrated in cultured cells (*4, 16*). Administration of TNF-α to otherwise normal humans or animals results in reductions in insulin sensitivity (*17*). Hence, it has become crucial to understand the detailed mechanisms of TNF-α action on IR signaling.

The IRS-1–mediated inhibition of IR tyrosine kinase activity could occur by direct or indirect interactions between the IR and IRS-1 (*18*). Serine-phosphorylated IRS-1 might associate with the IR in a manner that blocks the autophosphorylation reaction. Alternatively, serine-phosphorylated IRS-1 might act indirectly on the IR through an association with an inhibitor that acts on the IR in a stoichiometric or catalytic fashion. However, we have been unable to identify a distinct protein associated with IRS-1 from TNF-α–treated cells.

These results suggest an unexpected role for IRS-1 in insulin action. In addition to its function in the activation of downstream responses to insulin, IRS-1 appears to participate in the inhibition of insulin action. This raises the question of whether IRS-1 could play a role in the normal attenuation or termination of insulin action, outside the context of TNF-α or insulin resistance. IRS-1 is phosphorylated on serine and threonine residues, as well as tyrosine, upon insulin stimulation (*8*). It is possible that these phosphorylations serve to attenuate insulin action, before or after the key phosphotyrosines are removed by relevant tyrosine phosphatases. Finally, it is conceivable that the cross-talk between TNF-α and IR signaling is an example of a general regulatory cascade for molecules that use IRS-1 or related molecules in their signaling cascades (*15*).

REFERENCES AND NOTES

1. D. E. Moller and J. S. Flier, *N. Engl. J. Med.* **325**, 938 (1992).
2. G. S. Hotamisligil and B. M. Spiegelman, *Diabetes* **43**, 1271 (1994).
3. D. E. Moller, *Insulin Resistance* (Wiley, London, 1993); J. M. Olefsky and J. M. Molina, in *Diabetes Mellitus*, H. Rifkin and D. J. Porte, Eds. (Elsevier, New York, 1990), pp. 121–153.
4. G. S. Hotamisligil, N. S. Shargill, B. M. Spiegelman, *Science* **259**, 87 (1993).
5. C. Hofmann *et al.*, *Endocrinology* **134**, 264 (1994).
6. G. S. Hotamisligil, P. Arner, J. F. Caro, R. L. Atkinson, B. M. Spiegelman, *J. Clin. Invest.* **95**, 2409 (1995); P. A. Kern *et al.*, *ibid.*, p. 2111.

7. G. S. Hotamisligil, A. Budavari, D. L. Murray, B. M. Spiegelman, *ibid.* **94**, 1543 (1994).
8. M. F. White and C. R. Kahn, *J. Biol. Chem.* **269**, 1 (1994).
9. G. S. Hotamisligil, D. L. Murray, L. N. Choy, B. M. Spiegelman, *Proc. Natl. Acad. Sci. U.S.A.* **91**, 4854 (1994).
10. R. Feinstein, H. Kanety, M. Z. Papa, B. Lunenfeld, A. Karasik, *J. Biol. Chem.* **268**, 26055 (1993).
11. N. Begum, *Diabetes* **44**, 140A (1995); G. Kroder, M. Kellerer, B. Bossenmaier, A. Mühlhöfer, H.-U. Haring, *ibid.*, p. 264A.
12. G. S. Hotamisligil, P. Peraldi, B. M. Spiegelman, unpublished observations.
13. J. Vilcek and T. H. Lee, *J. Biol. Chem.* **266**, 7313 (1991).
14. J. F. Tanti, T. Gremeaux, E. Van Obberghen, Y. Le Marchand-Brustel, *ibid.* **269**, 6051 (1994).
15. L.-M. Wang *et al.*, *EMBO J.* **11**, 4899 (1992); L.-M. Wang *et al.*, *Science* **261**, 1591 (1993); X. L. Sun *et al.*, *Nature* **377**, 173 (1995).
16. J. M. Stephens and P. H. Pekala, *J. Biol. Chem.* **266**, 21839 (1991).
17. R. G. Douglas *et al.*, *Am. J. Physiol.* **261**, 606 (1991); T. Van Der Poll *et al.*, *ibid.*, p. E457; C. H. Lang, C. Dobrescu, G. J. Bagby, *Endocrinology* **130**, 43 (1992).
18. J. M. Backer *et al.*, *J. Biol. Chem.* **268**, 8204 (1993); T. J. O'Neill, A. Craparo, T. A. Gustafson, *Mol. Cell. Biol.* **14**, 6433 (1994).
19. After complete differentiation, adipocytes were treated with murine TNF-α (3 ng/ml; Genzyme) for 4 days in Dulbecco's modified Eagle's medium (DMEM) containing fetal calf serum (10%) and insulin (100 ng/ml; Sigma). On day 4, cells were washed twice in phosphate-buffered saline (PBS) and incubated in serum-free DMEM containing the same dose of TNF-α for 16 hours. The medium was then changed to phosphate-free medium with TNF-α but without serum. After 1 hour of incubation in this medium, [^{32}P]orthophosphate (3 mCi/ml, 6000 Ci/mmol; New England Nuclear) was added and incubation was continued for 3 hours at 37°C. Insulin stimulations were done by adding insulin (100 ng/ml) directly to the medium. Plates were washed with ice-cold PBS once and protein extracts were prepared as described. Immunoprecipitations were done from control and TNF-α–treated cells with polyclonal antibodies to IR and IRS-1 and a monoclonal antibody to phosphotyrosine in a 1:100 (v/v) dilution for 4 hours and analyzed by SDS–polyacrylamide gel electrophoresis (PAGE) and autoradiography.
20. W. J. Boyle, P. van der Geer, T. Hunter, *Methods Enzymol.* **201**, 110 (1991).
21. Specific pathogen-free, male Zucker obese (fa/fa) rats and their lean controls (+/?) were purchased from Charles River Laboratories. On arrival, rats were housed for at least 1 week before the experimental procedures were begun and fed standard rodent chow and water ad libitum. After a 6-hour fast, rats were anesthetized with ketamine and xylasine (intramuscular), the abdominal cavity was opened, and fat (epididymal), muscle (hind limb), and liver tissues were removed and frozen immediately in liquid nitrogen. Frozen tissues were ground into a fine powder with a mortar and pestle and then homogenized with a Polytron homogenizer at 4°C in 6× the tissue volume of homogenization buffer [1% Triton X-100, 150 mM NaCl, 10 mM Hepes (pH 7.4), 250 mM sucrose, 10 mM EDTA, 10 mM EGTA, 10 mM benzamidine, 2 mM phenylmethylsulfonyl fluoride (PMSF), and aprotinin (100 μg/ml)]. All extracts were centrifuged at 12,000 rpm for 30 min at 4°C, and the supernatants were collected for further analysis. All animal procedures were in accordance with institutional guidelines.
22. We thank C. Carpenter for phosphoamino acid analysis, M. Myers Jr. and B. Cheatham for gifts of 32D cells and other reagents, and C. R. Kahn for reviewing the manuscript. Supported by a grant from the National Institutes of Health (DK 42539 to B.M.S.) and fellowships from the American Diabetes Association (G.S.H.) and from the Association pour la Recherché sur le Cancer and Juveniles Diabetes Foundation International (P.P.).

20 July 1995; accepted 31 October 1995

TECHNICAL COMMENTS

The Age of the Waiho Loop Glacial Event

George H. Denton and C. H. Hendy (*1*) cite evidence from a South Pacific island for global forcing of Younger Dryas climatic cooling. However, their interpretation of the data can be challenged; more likely, earlier interpretations (*2*) that the Franz Josef Glacier in New Zealand's Southern Alps advanced before Younger Dryas time are still valid.

Denton and Hendy derive a simple weighted mean age of 11,150 ± 14 ^{14}C years before present (B.P.) from 36 radiocarbon dates and accept this without statistical testing. Following recommended procedures (*3*, *4*) a mean age of 11,130 ± 20 ^{14}C years B.P. can be calculated, but applying the χ^2 test for comparing multiple radiocarbon dates (*3*, *4*) shows this is not a valid age. By rejecting those dates with the largest individual χ^2 values, a statistically more valid weighted mean age of 11,180 ± 20 can be calculated.

Denton and Hendy (*1*) allow for about 100 years of transport time before wood deposition by the glacier, and they reject earlier evidence of a local origin for the wood (*2*). Their model requires that a deposit with abundant wood fragments, some with bark attached (*2*), survived about 8 km of supraglacial transport in a high rainfall environment. This is highly unlikely, and a local origin for the wood would be more parsimonious. Furthermore, even if their model is accepted, allowing 100 years for transport is overly generous. At a modest glacier flow rate of 1 m per day, it would take only about 20 years for the wood to travel the suggested 8 km. Thus, it is more likely that the glacier deposited the dated material before 11,100 years B.P., probably around 11,150 to 11,180 ^{14}C years B.P.

Denton and Hendy suggest the Waiho Loop advance would have been widely represented in other valleys. However, no correlative of the Waiho Loop moraine is known from the western parts of the island (*5*). The physiographic setting of the moraine is not unique, and numerous valleys to the north and south should contain equivalent moraines, had they been deposited. This suggests it was a local event and not representative of a widespread advance of glaciers in the Southern Alps. This is not unusual, as in a similar setting in southern Chile, a glacier has advanced, but not surged, over 10 km down Seno Exmouth since 1940, while adjacent glaciers have been retreating.

Direct correlation of the Waiho Loop advance with initiation of Younger Dryas cooling is invalid as the climate change that led to the advance would have occurred before the advance itself, and thus before the initiation of Younger Dryas cooling. The most accurately dated direct evidence (*6*) for climatic oscillations around 11,000 ^{14}C years B.P. shows [converting calendar ages to ^{14}C ages (*4*)] that a pre–Younger Dryas warm peak occurred at around 11,100 ^{14}C years B.P., before full Younger Dryas conditions set in by 10,800 ^{14}C years B.P. Using the age of 11,180 ^{14}C years B.P., one can only conclude that the Waiho Loop glacial event and the climatic changes that triggered it were not coincident with Younger Dryas climate cooling in the North Atlantic region.

The interpretation of Denton and Hendy of a Younger Dryas age advance of Franz Josef Glacier is unwarranted and earlier suggestions (*2*) that the Waiho Loop moraine was constructed before Younger Dryas time remain the most secure interpretation of the data. Evidence from this site should not be used to demonstrate global forcing of the Younger Dryas cooling event.

M. C. G. Mabin
Department of Tropical Environment Studies and Geography, James Cook University of North Queensland, Townsville, Q4811, Australia

REFERENCES

1. G. H. Denton and C. H. Hendy, *Science* **264**, 1434 (1994).
2. J. H. Mercer, *N.Z. Geol. Geophys.* **31**, 95 (1988); P. Wardle, *N.Z. Bot.* **16**, 147 (1978).
3. G. K. Ward and S. R. Wilson, *Archaeometry* **20**, 19 (1978).
4. M. Stuiver and P. J. Reimer, *Radiocarbon* **31**, 215 (1993).
5. C. J. Burrows, *Palaeogeogr. Palaeoclimatol. Palaeoecol.* **27**, 287 (1979); A. F. Gellatly, T. J. H. Chinn, F. Rothlisberger, *Quat. Sci. Rev.* **7**, 227 (1988).
6. S. J. Johnsen *et al.*, *Nature* **359**, 311 (1992); R. B. Alley *et al.*, *ibid.* **362**, 527 (1993).

30 June 1995; accepted 22 August 1995